Published in final edited form as:
Circulation. 2012 November 13; 126(20): 2418–2427. doi:10.1161/CIRCULATIONAHA.112.125971.

Ribosomal Protein L17, RpL17, is an Inhibitor of Vascular Smooth Muscle Growth and Carotid Intima Formation

Elaine M. Smolock, Ph.D.[1,2,*], **Vyacheslav A. Korshunov, Ph.D.**[1,2], **Galina Glazko, Ph.D.**[3], **Xing Qiu, Ph.D.**[3], **Janice Gerloff, B.S.**[1,2], and **Bradford C. Berk, M.D., Ph.D.**[1,2]

[1]Aab Cardiovascular Research Institute, University of Rochester School of Medicine & Dentistry, Rochester, NY 14642

[2]Department of Medicine, University of Rochester School of Medicine & Dentistry, Rochester, NY 14642

[3]Department of Biostatistics and Computational Biology, University of Rochester School of Medicine & Dentistry, Rochester, NY 14642

Abstract

Background—Carotid intima-media thickening is associated with increased cardiovascular risk in humans. We discovered that intima formation and cell proliferation in response to carotid injury is greater in SJL/J (SJL) compared to C3HeB/FeJ (C3H/F) mice. The purpose of this study was to identify candidate genes contributing to intima formation.

Methods and Results—We performed microarray and bioinformatic analyses of carotid arteries from C3H/F and SJL mice. Kyoto Encyclopedia of Genes and Genomes (KEGG) analysis showed that the ribosome pathway was significantly up-regulated in C3H/F compared to SJL. Expression of a ribosomal protein, RpL17, was >40-fold higher in C3H/F carotids compared to SJL. Aortic vascular smooth muscle cells (VSMC) from C3H/F grew slower compared to SJL. To determine the role of RpL17 in VSMC growth regulation we analyzed the relationship between RpL17 expression and cell cycle progression. Cultured VSMC from mouse, rat, and human showed that RpL17 expression inversely correlated with growth as shown by decreased cells in S phase and increased cells in G_0/G_1. To prove that RpL17 acted as a growth inhibitor *in vivo* we used pluronic gel delivery of RpL17 siRNA to C3H/F carotid arteries. This resulted in an 8-fold increase in the number of proliferating cells. Furthermore, following partial carotid ligation in SJL mice, RpL17 expression in the intima and media decreased while the number of proliferating cells increased.

Conclusions—RpL17 acts as a VSMC growth inhibitor (akin to a tumor suppressor) and represents a potential therapeutic target to limit carotid intima-media thickening.

Keywords

Bioinformatics; Vascular smooth muscle; Ribosomal proteins; Cell growth; Proliferation

INTRODUCTION

Cardiovascular diseases such as atherosclerosis and restenosis are complex disorders determined by genetic and environmental causes[1]. However, the genetic mechanisms for

Correspondence: Elaine M. Smolock, Ph.D., Aab Cardiovascular Research Institute, 601 Elmwood Avenue, Box CVRI, Rochester, NY 14642, Phone: 585-276-9840, Fax: 585-273-1497, Elaine_Smolock@URMC.rochester.edu.

DISCLOSURES: None.

traits associated with cardiovascular diseases are not well understood. Systems-oriented genetic approaches that incorporate transcriptomic and bioinformatic analyses are valuable for advancements in understanding complex traits[2–5].

An intermediate trait of atherosclerosis that is highly predictive for cardiovascular events in humans is carotid intima-media thickening (IMT)[6–10]. Inbred mouse strains that exhibit phenotypic variations are commonly used to discover genetic differences underlying cardiovascular diseases. To study genes that influence IMT we developed a carotid IMT model in mice in which intima is induced by low blood flow[11]. We previously demonstrated using this model that there are strain dependent differences in intima thickening that vary significantly among inbred mice[12]. C3HeB/FeJ (C3H/F) mice were resistant to intima formation while SJL/J (SJL) mice exhibited a significant increase in intima thickening[12]. We also reported that SJL mice have increased cell proliferation as well as endothelial dysfunction that contribute to intima formation[13,14]. We mapped three QTLs for intima formation which we termed *I*ntima *m*odifier (*Im*) loci: *Im1* on chr2; *Im2* on chr11 and *Im3* on chr18[15]. These findings indicate that the intima trait is genetically determined.

Understanding the genetic contribution to cardiovascular disease can be done by transcriptomic analyses of vascular tissues in inbred mice. Such approaches have been important in demonstrating gene expression differences that explain C57BL/6J mouse susceptibility to atherosclerosis compared to C3H/HeJ mice[16]. Lutgens et al, demonstrated with gene profiling that atherogenesis highly correlated with increased expression of small inducible cytokines including monocyte chemoattractant protein (MCP)-1 between C3H/HeJ and C57BL/6J[17]. This finding was later strengthened by microarray and bioinformatic pathway analyses that found that alterations in calcium signaling contributed to the differences in MCP-1 production in these strains[18].

To identify candidate genes that might localize to our previously published *Im1, Im2* and *Im3* loci[15] we used a similar combinatorial approach of microarray and bioinformatic pathway analyses in C3H/F and SJL inbred mice. We confirmed some known pathways such as antigen presentation and processing in the immune pathway and discovered a new one, the ribosome pathway. We further validated and proposed a functional role for one specific gene in the ribosome pathway, ribosomal protein L17 (RpL17). Our data provides evidence that RpL17 is a vascular smooth muscle cell (VSMC) growth inhibitor, akin to a tumor suppressor. This finding is significant as it is the first to show that a ribosomal protein functions to inhibit VSMC cell cycle progression and growth, making it a potential therapeutic target to limit carotid IMT.

MATERIALS AND METHODS

Methods are expanded in Online Supplement

Animals and surgeries—Sham-operations and ligations on male mice from each strain (C3H/F and SJL) were performed as described[11]. Four groups of mice were examined: C3H/F shams (n=4), C3H/F ligated (n=5), SJL shams (n=4), and SJL ligated (n=5).

Microarray and KEGG analysis of carotid arteries—Carotids were harvested at day 14 after surgery and immediately frozen in liquid nitrogen for total RNA isolation using Qiagen RNAeasy Micro kit. RNA was processed to amplified cDNA using NuGen's Ovation RNA Amplification System V2 with final purification of the amplified cDNA done using the NucleoSpin Extract I kit. Fragmentation and biotinylation of the amplified cDNA was accomplished using NuGen's FL-Ovation cDNA Biotin Module V2 and hybridized to Affymetrix GeneChip M430 2.0 arrays. Washing, staining and scanning of these arrays was done using the Affymetrix FS-450 Fluidics station and the Affymetrix GeneChip Scanner

3000. Each array contained gene expression level information of 45,037 probe sets of the 39,000 known transcripts for 34,000 known or predicted mouse genes. The probe level data were assembled to a unique number representing the expression level by using the RMA preprocessing procedure, which is available in the BioConductor package[19] for R software[20]. We conducted the following sample comparisons to identify differentially expressed genes: 1) C3H/F shams vs. SJL shams; 2) C3H/F shams vs. C3H/F ligated; 3) SJL shams vs. SJL ligated; 4) C3H/F ligated vs. SJL ligated. For each comparison, we used the Delta-sequence method to select differentially expressed genes. The Delta-sequence method exploits a special structure in gene expression data that produces a sequence of weakly dependent random variables. This method has two distinct advantages. First, it leads to dramatic gains in terms of testing power, as well as in stability of the results of testing. Second, its outcomes are entirely free from the log-additive array-specific technical noise, so no normalization is needed. Therefore, in the current study, we used the Delta-sequence method (with the shift method) in conjunction with the two sample Student's t-statistics. Then, as in the global normalization method, we applied extended Bonferroni multiple testing procedure to select differentially expressed genes at per-family error rate level 10[21]. We compared gene sets using the Kyoto Encyclopedia of Genes and Genomes (KEGG) pathway analyses[22]. Using BioConductor package 'Category'[19] we mapped all KEGG pathways to genes in the Affymetrix M430 2.0 array. For every pathway we tested the hypothesis whether the pathway was differentially expressed between the two strains (C3H/F vs. SJL) using 'N-statistics'[23]. The complement of correlation coefficient between gene expression vectors was used as a distance measure. We then aimed to map differentially expressed genes to the intima QTLs[24] in KEGG pathways. To visualize gene expression in the ribosome pathway we constructed heatmaps representing hierarchical clustering of ribosomal protein gene expression vectors. The complement of correlation coefficient between gene expression vectors was used as a distance measure.

Pluronic gel delivery of siRNA *in vivo*—C3H/F male mice were anesthetized as described[11]. Pluronic gel (BASF F127, Prill) was made as a 4% solution (2g dissolved in 5mL ice cold sterile phosphate buffered solution) and kept on ice. Application of pluronic gel was done similarly as described[25]. Carotid arteries were isolated by gently dissecting the common carotids free of connective tissue. A 6.0 silk suture was placed beneath the common carotid and gently used to lift the carotid out of the neck cavity. 25μL of ice cold pluronic gel containing either scrambled siRNA (siScr) (100nM) or RpL17 siRNA (siRpL17) (100nM) (Santa Cruz Biotechnology, Inc) was applied to the neck cavity, suture removed to release the carotid back into the neck and another 25μL of pluronic gel containing siRNA applied to the top of the carotid. siRpL17 was applied to the left carotid and siScr to the contralateral right carotid, as an internal control. The incision was sutured and mice were individually housed and allowed to recover. Carotid arteries were harvested at days 0, 1, 3 and 7 following siRNA delivery. RpL17 knockdown was greatest at day 3. At day 7 following siRNA delivery RpL17 levels returned to those observed at day 0.

Carotid ligation and immunohistochemistry—Ligations of carotid arteries in male mice from C3H/F and SJL were performed as described[11]. Carotid arteries were harvested 7 days after surgery. Mice were perfused and fixed in 4% paraformaldehyde and vessels paraffin embedded. Sections were deparaffinized and rehydrated in Tris buffered solution (TBS). Slides were incubated in 3% H_2O_2 and washed with TBS. Antigen retrieval was done using HEIR 10mM citrate buffer (pH 6.0) followed by washing in TBS. Sections were blocked with 5% normal horse serum (DakoCytomation) for 30 min followed by primary RpL17 antibody (Everest Biotech Ltd; 1:1000 in Dako antibody dilutent) for 60 min. Normal goat IgG (Santa Cruz Biotechnology, Inc) was used as a negative control (1:1000). For RpL17 sections were washed with TBS and incubated in secondary biotinylated horse

anti-goat IgG antibody with the Vectastain ABC kit (PK-6100, Vector Laboratories, Inc.) (1:500) for 30 min. For proliferating cell nuclear antigen (PCNA) sections were blocked in Dako antibody dilutent followed by PCNA (Thermo Scientific) (1:500) overnight at 4°C. Protein was detected using Liquid DAB+substrate Chromogen system (DakoCytomation) and counterstained with hemathoyxlin. Slides were imaged using an Olympus BX41 microscope with digital camera at 60X (Spot Insight 2, Diagnostic Instruments, INC). Quantification was done using ImagePro Plus software as described previously[26]. For each image a pixel threshold was set for nuclei in the medial and intimal area. This allowed the software to provide a total cell number count. A second measurement for the same area was acquired using an adjusted pixel threshold for cells staining positively for RpL17 and PCNA.

Statistical Analyses

Microarray statistical analysis is described in detail above. In all other experiments where data sets from greater than two groups were being compared a one-way ANOVA was used. In cases where only two groups were being compared a Student's t-test was used.

RESULTS

Microarray and KEGG analyses between carotids from mouse strains

We performed a microarray of 34,000 genes and found 276 differentially expressed transcripts in the carotids of C3H/F mice compared to SJL mice. (Supplemental Tables S1–S8 show the complete list of genes that differed between groups). We arranged the complete list of 276 genes from our microarray analyses into pathways using KEGG to look for significant differences in pathways. We used KEGG because it has the ability to reduce the number of testable pathways and gene candidates between mouse strains. Using the KEGG database we found 4 categories (including 15 pathways) that were differentially expressed between C3H/F and SJL carotids (Table 1). The four categories were: metabolism, genetic information and processing, cellular process, and human disease. Accordingly, the KEGG analysis confirmed our previously reported difference in the immune pathway[13] (sub-category of cellular process in Table 1) and also identified novel pathways that included differentially expressed genes from the microarray analysis. Several genes identified in the microarray fell into KEGG pathways that likely contribute to the intima trait (Supplemental Table S9). These include: Casp9 (involved in apoptosis and fits our previous observations of dramatic differences in apoptosis between remodeled C3H/F and SJL carotid arteries[13]), Dclre1c (Artemis) (immunodeficiency pathway), CD47 (receptor in extracellular matrix-receptor interactions), Frz4 (involved in the WNT-signaling pathway), Smurf2 (TGF- signaling), IRF3 (toll-like receptor signaling), Nln (renin-angiotensin system), Serpin1b (complement and coagulation cascades), PRP19 (ubiquitin-mediated pathways) and our prime candidate, RpL17 (component of the large 60S ribosome). Among these genes RpL17 was the only one that was significantly different between strain comparison as well as in sham and ligated comparisons (Supplemental Tables S1 and S8). We also performed cluster analysis of ribosomal proteins and found that RpL17 expression was higher in all C3H/F mice compared to SJL (Supplemental Fig. 1). Thus, we identified important genes and pathways whose expression differed significantly in carotid arteries between C3H/F and SJL mice.

Validation of differences in RpL17 expression

We chose to further validate RpL17 because of its significant difference in gene expression from the microarray, representation in KEGG pathways analysis (Supplemental Table S4) and heatmap analysis (Supplemental Fig. 1) and location relative to the *Im*3 locus on chr18. We performed quantitative (q)RT-PCR for RpL17 expression in C3H/F and SJL carotid

arteries. There was a significant increase in RpL17 expression in C3H/F in both shams (50-fold) and after ligation (41-fold) compared to SJL (Fig. 1A). We used cultured mouse aortic smooth muscle cells (MASMC) from C3H/F and SJL aortas to establish a model to analyze the functional consequences of differences in RpL17 expression. We focused on cell growth because we previously showed that in response to low flow C3H/F carotids exhibit dramatically less proliferation compared to SJL[13]. We found that C3H/F MASMC grew significantly slower compared to SJL MASMC (Fig. 1B), consistent with the *in vivo* cell proliferation data[13]. Importantly, qRT-PCR demonstrated that RpL17 expression in MASMC was >6-fold higher in C3H/F compared to SJL at passage 4 (Fig. 1C). We also measured RpL17 protein expression in MASMC. The representative immunoblot (Fig. 1D) shows the magnitude of increase (~2.5-fold) in RpL17 expression in C3H/F compared to SJL MASMC. Similarly, we found that RpL17 protein expression was greater in C3H/F aortas compared to SJL aortas (Supplemental Fig. 2).

Cell cycle analysis reveals increased S phase in SJL MASMC

Our *in vitro* MASMC model confirmed that VSMC from C3H/F grow slower compared to SJL (Fig. 1B). By propidium iodide staining and flow cytometry we characterized cell cycle as shown in Figure 2. MASMC from C3H/F were primarily arrested in G_0/G_1 phase, while SJL exhibited a dramatic increase in percentage of cells in S phase (Fig. 2A–C; Supplemental Table S10). A specific comparison at basal (0 hrs) and after 24 hrs of serum stimulation revealed a significant increase in the percentage of cells in S phase relative to G_0/G_1 in SJL MASMC compared to C3H/F. To confirm these cell cycle differences we used cyclin D1, a cell cycle dependent kinase often measured as an index of cell cycle progression[27]. There was a dramatic difference in cyclin D1 expression, with higher levels in SJL MASMC compared to C3H/F, especially at 24 hrs (Fig. 2D). These data strongly support our previous findings that SJL VSMC are highly proliferative compared to C3H/F.

RpL17 depletion *in vitro* increases VSMC proliferation

To determine whether changes in RpL17 expression altered cell cycle, we depleted RpL17 in VSMC. siRNA mediated knockdown of RpL17 significantly decreased its expression in rat aortic vascular smooth muscle cells (RASMC) (Fig. 3A). After 24 hrs of serum stimulation, RASMC deficient in RpL17 had a significant increase in the ratio of cells in S phase relative to G_0/G_1, similar to the cell cycle data for SJL (Fig. 3B–C; Supplemental Table 11). We also found that decreasing RpL17 mRNA in human aortic vascular smooth muscle cells (HASMC) resulted in an increase in cells in S phase compared to G_0/G_1 (Supplemental Fig. 3; Supplemental Table S12). Thus, we used three different *in vitro* VSMC lines, mouse, rat and human, and demonstrated that RpL17 regulates VSMC cell cycle, especially progression to S phase.

Previously we showed that after carotid ligation C3H/F intima exhibited more apoptotic cells compared to SJL[13]. Ribosomal proteins have been shown to be mediators of apoptosis. For example, overexpression of RpL7 in T-lymphoma cells[28] and RpS3a in tumor cells[29] can induce apoptosis. Therefore, we investigated if RpL17 expression affected apoptosis. Using flow cytometric analysis with Annexin V and propidium iodide staining we found no effect on apoptosis or necrosis when RpL17 expression was decreased by siRpL17 (Fig. 4; Supplemental Fig. 4). These findings suggest that RpL17's predominant role is to regulate VSMC growth and not apoptosis.

RpL17 depletion *in vivo* increases VSMC proliferation

To determine if changes in RpL17 expression are sufficient to alter cell proliferation *in vivo* we decreased RpL17 expression using pluronic gel delivery of siRpL17 in C3H/F left carotid arteries (Fig. 5). As an internal control siScr was applied to the contralateral right

carotid arteries of all animals. After 3 days of siRNA delivery we harvested carotids and immunostained for RpL17 and PCNA in serial sections. In the control (siScr) right carotids there was no effect on RpL17 expression (Fig 5A–B; inserts) or PCNA expression (Fig 5C–D; inserts). However, with siRpL17 in the left carotids we showed an ~2.5-fold decrease in cells expressing RpL17 (Fig. 5A–B, quantified in 5E) that correlated with an ~8-fold increase in PCNA expression (Fig. 5C–D; quantified in 5F). This data shows that decreasing RpL17 expression in the carotid artery increases proliferation of medial VSMC. This finding is highly significant because it indicates that RpL17 is a VSMC growth inhibitor *in vivo* (akin to a tumor suppressor).

Intimal proliferating cells have decreased RpL17 expression

We demonstrated that depletion of RpL17 increased VSMC proliferation *in vivo* (Fig. 5). We have previously shown that SJL carotids have an increased number of proliferating cells in the intima compared to C3H/F in response to low blood flow[13]. To determine whether this increase in the number of proliferating cells was a result of a decreased number of RpL17 expressing cells we immunostained carotids from C3H/F and SJL 7 days following partial carotid ligation (Fig. 6). Immunohistochemistry showed greater RpL17 protein expression in C3H/F (Fig. 6A) compared to SJL (Fig. 6B). PCNA staining in serial sections indicated that SJL cells (Fig. 6C) were more proliferative compared to C3H/F (Fig. 6D). RpL17 and PNCA expressing cells were quantified relative to the total number of cells in the intima and media (Fig. 6E–F). We found that there is an inverse relationship between RpL17 expression and cell proliferation. In particular, in SJL the number of RpL17 expressing cells was decreased and PCNA expressing cells was increased after one week of injury. Thus, our *in vivo* data support a role for RpL17 in the regulation of intima and media cell proliferation.

DISCUSSION

The major finding of this study is the identification of RpL17 as a novel vascular smooth cell growth inhibitor. Specifically, we showed that 1) the ribosome pathway is a key mediator of carotid intima formation in response to injury, 2) RpL17 can maintain VSMC in G_0/G_1 and inhibit growth in three *in vitro* cell lines, 3) decreasing levels of RpL17 expression specifically with siRNA *in vivo* caused cell proliferation, and 4) following injury the intima and media of SJL carotids have decreased RpL17 expressing cells and an increased number of proliferating cells. Our data provide strong evidence for a functional role of RpL17 in VSMC mediated intima formation. This study is important because it is the first to show that a ribosomal protein can function to prevent VSMC cell cycle progression, similar to tumor suppressor genes, while having no effect on cell apoptosis. Thus, a ribosomal protein, RpL17, is a novel VSMC growth regulator that warrants further investigation in vascular biology.

Carotid IMT is a complex multigenetic trait that is highly predictive for cardiovascular events. We used a microarray and bioinformatic approach to identify candidate genes for IMT. Such approaches have been useful in identifying causal genes for complex cardiovascular diseases. For example, using microarray with likelihood-based causality model selection and comparative human genome wide association studies it was reported that *C3ar1* is a causal gene for aortic lesion development in an atherosclerotic mouse model[30]. Another recent study used tagged single nucleotide polymorphism mapping in combination with microarray and gene pathway analyses of cultured VSMC to identify *Id3* as having a functional role in regulating IMT[31]. In our study we used KEGG to narrow our microarray gene list. We identified a number of genes that are involved in pathways already likely to play a role in intima formation and one novel candidate. Three of the identified genes localized to our QTLs for strain dependent intima formation[15]: Dclre1c (*Im*1),

Serpin1b (*Im*2) and RpL17 (*Im*3). Given the already known roles for Dclre1c and Serpin1b, we chose to focus on RpL17. Interestingly, RpL17 was the only gene whose expression differed significantly between strains in both sham and ligated carotids. This makes RpL17 a strong novel candidate. We present functional data that implicates RpL17 as having a significant role in influencing the intima trait via regulation of VSMC growth.

We observed that MASMC from C3H/F grew significantly slower compared to SJL. This is consistent with a previous finding which showed that VSMC from another C3H substrain, C3H/HeJ, grew more slowly compared to cells isolated from FVB/NJ mice[32]. Like SJL, FVB/NJ mice exhibit greater intima formation in response to low blood flow[12,32]. The decreased growth rate in C3H/F MASMC appears to be related to changes in cell cycle, since C3H/F cells arrested in G_0/G_1 had higher levels of RpL17 compared to SJL MASMC. This conclusion is supported by a previous study demonstrating that over-expression of RpL7 in T-lymphocytes promoted G_0/G_1 arrest[28]. In contrast to C3H/F, SJL MASMC are more proliferative as evidenced by the high ratio of cells in S phase compared to G_0/G_1. Importantly, we also found that depletion of RpL17 in both rat and human VSMCs phenocopied the SJL cell cycle distribution, strongly supporting a role for RpL17 as a key contributing regulatory factor for VSMC cell cycle progression. Consistent with the *in vitro* RpL17 depletion results, we found that decreasing RpL17 expression in C3H/F carotids resulted in increased cell proliferation. Furthermore, we found a significant increase in RpL17 expressing cells relative to proliferating cells in the intima of C3H/F mice following injury. Conversely, in SJL there was a decrease in RpL17 expressing cells and an increase in cell proliferation. This collective data strongly indicates that RpL17 can function like a tumor suppressor. Because we saw no effect on apoptosis *in vitro* following RpL17 depletion it is probable that VSMC proliferation is more dependent on RpL17's regulation of cell growth and proliferation and not apoptosis. Thus, we would propose that candidate genes other than RpL17, most likely those present in the *Im*1 and *Im*2 loci, are involved in the apoptotic pathways observed in C3H/F carotids[13].

While RpL17 is part of the translational machinery it is possible that its inhibitory effect on growth may exist outside of the ribosome (extra-ribosomal) to alter cellular processes such as cell cycle and gene transcription[33–35]. Some diseases involving dysfunctions in cell cycle and growth have been directly attributed to deletions or mutations in ribosomal proteins. Mutations in RpS14 are related to 5q-syndrome[36] and RpS19 and RpS35a deficiencies result in Diamond-Blackfan anemia[37]. Interesting, as in our study, RpS35a was identified in the anemic disorder using genomic mapping and microarray analysis[37]. Ribosomal proteins are also differentially expressed in colorectal[38], gastric[39], nasopharyngeal[40] and prostate[41] cancers. Specific ribosomal proteins have been to shown to function in an extra-ribosomal manner as either tumor promoters (RpL19)[41] or tumor suppressors (RpL5, RpL11 and RpL23 (which is the human homolog for RpL17)[35,39,42]. RNAi mediated knockdown of RpL19 in a prostate cell line (PC-3M cells) emphasized the importance of RpL19 in inhibiting the transformation of benign cells to malignant ones[41]. Relevant to our findings, studies using an osteosarcoma cell line demonstrated that RpL5 and RpL11 cooperatively act to increase G_1 arrest[42–46]. Tumors that are deficient in one or both of these ribosomal proteins have increased cell growth[46, 47]. Our results strongly suggest that RpL17 may serve an extra-ribosomal function as a tumor suppressor gene in VSMC, opening novel avenues of mechanistic investigation into the regulation of VSMC growth by RpL17, which could be applicable to not only carotid intima thickening but possibly angiogenesis.

Since intima is a complex trait we acknowledge that other pathways and candidate genes should be considered in future studies. The KEGG analysis identified significant differences in the antigen processing and presentation pathways, confirming our previous findings that the inflammatory response contributes significantly to intima thickening[13,26,48]. We

previously demonstrated that cytokines IL-18 and MIF were differentially expressed between C3H/F and SJL carotids[13] and that SJL mice have endothelial dysfunction[14]. A recent study showed that a ribosomal protein, RpS19, colocalized and interacted with MIF resulting in a decreased inflammatory response in aortic endothelial cells[49]. Thus, there could be a potential for interplay between pathways such that ribosomal proteins may play a role in regulating inflammation and vascular wall responses associated with intima formation.

We acknowledge there are limitations to our study. While we demonstrated that local knockdown of RpL17 in the carotid artery under basal conditions results in an increase in the number of proliferating cells, it would be interesting to see what effect RpL17 knockdown has on intima formation following carotid ligation. However, we observed that at 7 days after ectopic delivery of siRpL17 the number of RpL17 expressing cells returned to levels observed at day 0 (data not shown), indicating a potential time dependent effect. Thus, there are technical difficulties in long term siRNA mediated knockdown. Additionally, since intima formation is a polygenic trait it is likely that there will also be contribution from the *Im*1 and *Im*2 loci. In our future studies we are creating congenic mice for our three previously published QTLs (*Im*1, *Im*2 and *Im*3) using approximately 4000 SNPs that differ between SJL and C3H/F mice. RpL17 resides on chr18 near the *Im*3 locus. Introgressing chr18 segments from the SJL mouse on the C3H/F background will provide the ability to directly investigate the effects of RpL17 on intima formation as well as the percent contribution attributable to the locus and the gene.

In summary we identified a role for RpL17 as a novel inhibitor of vascular smooth muscle cell growth (akin to a tumor suppressor), providing a potential therapeutic target for carotid IMT with potential applicability to angiogenesis in humans.

Supplementary Material

Refer to Web version on PubMed Central for supplementary material.

Acknowledgments

We would like to thank: Michelle Zanche and Stephen Welle, Ph.D., in the Functional Genomics Core and Timothy Bushnell, Ph.D., in the Flow Cytometry Core at the University of Rochester School of Medicine. We extend our thanks to Audrey Ponce De Leon in the Flow Cytometry Core at The Methodist Hospital.

FUNDING SOURCES: This study was supported by NIH HL-62826 to B.C.B. and by an NRSA HL093986 awarded to E.M.S.

References

1. Lusis AJ, Pajukanta P. A treasure trove for lipoprotein biology. Nat Genet. 2008; 40:129–130. [PubMed: 18227868]
2. Thongboonkerd V. Genomics, proteomics and integrative “omics” in hypertension research. Curr Opin Nephrol Hypertens. 2005; 14:133–139. [PubMed: 15687839]
3. Schadt EE, Lamb J, Yang X, Zhu J, Edwards S, Guhathakurta D, Sieberts SK, Monks S, Reitman M, Zhang C, Lum PY, Leonardson A, Thieringer R, Metzger JM, Yang L, Castle J, Zhu H, Kash SF, Drake TA, Sachs A, Lusis AJ. An integrative genomics approach to infer causal associations between gene expression and disease. Nat Genet. 2005; 37:710–717. [PubMed: 15965475]
4. Mehrabian M, Allayee H, Stockton J, Lum PY, Drake TA, Castellani LW, Suh M, Armour C, Edwards S, Lamb J, Lusis AJ, Schadt EE. Integrating genotypic and expression data in a segregating mouse population to identify 5-lipoxygenase as a susceptibility gene for obesity and bone traits. Nat Genet. 2005; 37:1224–1233. [PubMed: 16200066]

5. Seda O, Tremblay J, Gaudet D, Brunelle PL, Gurau A, Merlo E, Pilote L, Orlov SN, Boulva F, Petrovich M, Kotchen TA, Cowley AW Jr, Hamet P. Systematic, genome-wide, sex-specific linkage of cardiovascular traits in french canadians. Hypertension. 2008; 51:1156–1162. [PubMed: 18259002]
6. Allan PL, Mowbray PI, Lee AJ, Fowkes FG. Relationship between carotid intima-media thickness and symptomatic and asymptomatic peripheral arterial disease. The edinburgh artery study. Stroke. 1997; 28:348–353. [PubMed: 9040688]
7. Davis PH, Dawson JD, Riley WA, Lauer RM. Carotid intimal-medial thickness is related to cardiovascular risk factors measured from childhood through middle age: The muscatine study. Circulation. 2001; 104:2815–2819. [PubMed: 11733400]
8. Cheng Y, Austin SC, Rocca B, Koller BH, Coffman TM, Grosser T, Lawson JA, FitzGerald GA. Role of prostacyclin in the cardiovascular response to thromboxane a2. Science. 2002; 296:539–541. [PubMed: 11964481]
9. Lorenz MW, Markus HS, Bots ML, Rosvall M, Sitzer M. Prediction of clinical cardiovascular events with carotid intima-media thickness: A systematic review and meta-analysis. Circulation. 2007; 115:459–467. [PubMed: 17242284]
10. Lorenz MW, Karbstein P, Markus HS, Sitzer M. High-sensitivity c-reactive protein is not associated with carotid intima-media progression: The carotid atherosclerosis progression study. Stroke. 2007; 38:1774–1779. [PubMed: 17446427]
11. Korshunov VA, Berk BC. Flow-induced vascular remodeling in the mouse: A model for carotid intima-media thickening. Arterioscler Thromb Vasc Biol. 2003; 23:2185–2191. [PubMed: 14576075]
12. Korshunov VA, Berk BC. Strain-dependent vascular remodeling: The “glagov phenomenon” is genetically determined. Circulation. 2004; 110:220–226. [PubMed: 15226209]
13. Korshunov VA, Nikonenko TA, Tkachuk VA, Brooks A, Berk BC. Interleukin-18 and macrophage migration inhibitory factor are associated with increased carotid intima-media thickening. Arterioscler Thromb Vasc Biol. 2006; 26:295–300. [PubMed: 16293799]
14. Chen C, Korshunov VA, Massett MP, Yan C, Berk BC. Impaired vasorelaxation in inbred mice is associated with alterations in both nitric oxide and super oxide pathways. J Vasc Res. 2007; 44:504–512. [PubMed: 17664889]
15. Korshunov VA, Berk BC. Genetic modifier loci linked to intima formation induced by low flow in the mouse carotid. Arterioscler Thromb Vasc Biol. 2009; 29:47–53. [PubMed: 18948632]
16. Shi W, Wang NJ, Shih DM, Sun VZ, Wang X, Lusis AJ. Determinants of atherosclerosis susceptibility in the c3h and c57bl/6 mouse model: Evidence for involvement of endothelial cells but not blood cells or cholesterol metabolism. Circ Res. 2000; 86:1078–1084. [PubMed: 10827138]
17. Lutgens E, Faber B, Schapira K, Evelo CT, van Haaften R, Heeneman S, Cleutjens KB, Bijnens AP, Beckers L, Porter JG, Mackay CR, Rennert P, Bailly V, Jarpe M, Dolinski B, Koteliansky V, de Fougerolles T, Daemen MJ. Gene profiling in atherosclerosis reveals a key role for small inducible cytokines: Validation using a novel monocyte chemoattractant protein monoclonal antibody. Circulation. 2005; 111:3443–3452. [PubMed: 15967845]
18. Yuan Z, Pei H, Roberts DJ, Zhang Z, Rowlan JS, Matsumoto AH, Shi W. Quantitative trait locus analysis of neointimal formation in an intercross between c57bl/6 and c3h/hej apolipoprotein e-deficient mice. Circ Cardiovasc Genet. 2009; 2:220–228. [PubMed: 19718279]
19. Gentleman RC, Carey VJ, Bates DM, Bolstad B, Dettling M, Dudoit S, Ellis B, Gautier L, Ge Y, Gentry J, Hornik K, Hothorn T, Huber W, Iacus S, Irizarry R, Leisch F, Li C, Maechler M, Rossini AJ, Sawitzki G, Smith C, Smyth G, Tierney L, Yang JY, Zhang J. Bioconductor: Open software development for computational biology and bioinformatics. Genome Biol. 2004; 5:R80. [PubMed: 15461798]
20. Team RDC. A language and environment for statistical computing. R Foundation for Statistical Computing; VIenna, Austria: 2006.
21. Gordon A, Glazko G, Qiu X, Yakovlev AY. Control of the mean number of false discoveries, bonferroni, and stability of multiple testing. Ann Appl Stat. 2007; 1:179–190.

22. Kanehisa M, Goto S. Kegg: Kyoto encyclopedia of genes and genomes. Nucleic Acids Res. 2000; 28:27–30. [PubMed: 10592173]
23. Kong SW, Pu WT, Park PJ. A multivariate approach for integrating genome-wide expression data and biological knowledge. Bioinformatics. 2006; 22:2373–2380. [PubMed: 16877751]
24. Korshunov VA, Berk BC. Smooth muscle apoptosis and vascular remodeling. Curr Opin Hematol. 2008; 15:250–254. [PubMed: 18391793]
25. Chiang HY, Korshunov VA, Serour A, Shi F, Sottile J. Fibronectin is an important regulator of flow-induced vascular remodeling. Arterioscler Thromb Vasc Biol. 2009; 29:1074–1079. [PubMed: 19407246]
26. Satoh K, Matoba T, Suzuki J, O'Dell MR, Nigro P, Cui Z, Mohan A, Pan S, Li L, Jin ZG, Yan C, Abe J, Berk BC. Cyclophilin a mediates vascular remodeling by promoting inflammation and vascular smooth muscle cell proliferation. Circulation. 2008; 117:3088–3098. [PubMed: 18541741]
27. Nagel DJ, Aizawa T, Jeon KI, Liu W, Mohan A, Wei H, Miano JM, Florio VA, Gao P, Korshunov VA, Berk BC, Yan C. Role of nuclear ca2+/calmodulin-stimulated phosphodiesterase 1a in vascular smooth muscle cell growth and survival. Circ Res. 2006; 98:777–784. [PubMed: 16514069]
28. Neumann F, Krawinkel U. Constitutive expression of human ribosomal protein l7 arrests the cell cycle in g1 and induces apoptosis in jurkat t-lymphoma cells. Exp Cell Res. 1997; 230:252–261. [PubMed: 9024784]
29. Naora H, Takai I, Adachi M. Altered cellular responses by varying expression of a ribosomal protein gene: Sequential coordination of enhancement and suppression of ribosomal protein s3a gene expression induces apoptosis. J Cell Biol. 1998; 141:741–753. [PubMed: 9566973]
30. Yang X, Peterson L, Thieringer R, Deignan JL, Wang X, Zhu J, Wang S, Zhong H, Stepaniants S, Beaulaurier J, Wang IM, Rosa R, Cumiskey AM, Luo JM, Luo Q, Shah K, Xiao J, Nickle D, Plump A, Schadt EE, Lusis AJ, Lum PY. Identification and validation of genes affecting aortic lesions in mice. J Clin Invest. 2010; 120:2414–2422. [PubMed: 20577049]
31. Doran AC, Lehtinen AB, Meller N, Lipinski MJ, Slayton RP, Oldham SN, Skaflen MD, Yeboah J, Rich SS, Bowden DW, McNamara CA. Id3 is a novel atheroprotective factor containing a functionally significant single-nucleotide polymorphism associated with intima-media thickness in humans. Circ Res. 2010; 106:1303–1311. [PubMed: 20185798]
32. Harmon KJ, Couper LL, Lindner V. Strain-dependent vascular remodeling phenotypes in inbred mice. Am J Pathol. 2000; 156:1741–1748. [PubMed: 10793085]
33. Wool IG. Extraribosomal functions of ribosomal proteins. Trends Biochem Sci. 1996; 21:164–165. [PubMed: 8871397]
34. Lindstrom MS. Emerging functions of ribosomal proteins in gene-specific transcription and translation. Biochem Biophys Res Commun. 2009; 379:167–170. [PubMed: 19114035]
35. Warner J, McIntosh K. How common are extraribosomal functions of ribosomal proteins? Molecular Cell Review. 2009; 34:3–11.
36. Ebert BL, Pretz J, Bosco J, Chang CY, Tamayo P, Galili N, Raza A, Root DE, Attar E, Ellis SR, Golub TR. Identification of rps14 as a 5q- syndrome gene by rna interference screen. Nature. 2008; 451:335–339. [PubMed: 18202658]
37. Farrar JE, Nater M, Caywood E, McDevitt MA, Kowalski J, Takemoto CM, Talbot CC Jr, Meltzer P, Esposito D, Beggs AH, Schneider HE, Grabowska A, Ball SE, Niewiadomska E, Sieff CA, Vlachos A, Atsidaftos E, Ellis SR, Lipton JM, Gazda HT, Arceci RJ. Abnormalities of the large ribosomal subunit protein, rpl35a, in diamond-blackfan anemia. Blood. 2008; 112:1582–1592. [PubMed: 18535205]
38. Kobayashi T, Sasaki Y, Oshima Y, Yamamoto H, Mita H, Suzuki H, Toyota M, Tokino T, Itoh F, Imai K, Shinomura Y. Activation of the ribosomal protein l13 gene in human gastrointestinal cancer. Int J Mol Med. 2006; 18:161–170. [PubMed: 16786168]
39. Lai MD, Xu J. Ribosomal proteins and colorectal cancer. Curr Genomics. 2007; 8:43–49. [PubMed: 18645623]

40. Sim EU, Ang CH, Ng CC, Lee CW, Narayanan K. Differential expression of a subset of ribosomal protein genes in cell lines derived from human nasopharyngeal epithelium. J Hum Genet. 2010; 55:118–120. [PubMed: 19927161]
41. Bee A, Brewer D, Beesley C, Dodson A, Forootan S, Dickinson T, Gerard P, Lane B, Yao S, Cooper CS, Djamgoz MB, Gosden CM, Ke Y, Foster CS. Sirna knockdown of ribosomal protein gene rpl19 abrogates the aggressive phenotype of human prostate cancer. PLoS One. 2011; 6:e22672. [PubMed: 21799931]
42. Dai MS, Zeng SX, Jin Y, Sun XX, David L, Lu H. Ribosomal protein l23 activates p53 by inhibiting mdm2 function in response to ribosomal perturbation but not to translation inhibition. Mol Cell Biol. 2004; 24:7654–7668. [PubMed: 15314173]
43. Lohrum MA, Ludwig RL, Kubbutat MH, Hanlon M, Vousden KH. Regulation of hdm2 activity by the ribosomal protein l11. Cancer Cell. 2003; 3:577–587. [PubMed: 12842086]
44. Zhang Y, Wolf GW, Bhat K, Jin A, Allio T, Burkhart WA, Xiong Y. Ribosomal protein l11 negatively regulates oncoprotein mdm2 and mediates a p53-dependent ribosomal-stress checkpoint pathway. Mol Cell Biol. 2003; 23:8902–8912. [PubMed: 14612427]
45. Takagi M, Absalon MJ, McLure KG, Kastan MB. Regulation of p53 translation and induction after DNA damage by ribosomal protein l26 and nucleolin. Cell. 2005; 123:49–63. [PubMed: 16213212]
46. Horn HF, Vousden KH. Cooperation between the ribosomal proteins l5 and l11 in the p53 pathway. Oncogene. 2008; 27:5774–5784. [PubMed: 18560357]
47. Bhat KP, Itahana K, Jin A, Zhang Y. Essential role of ribosomal protein l11 in mediating growth inhibition-induced p53 activation. Embo J. 2004; 23:2402–2412. [PubMed: 15152193]
48. Tanaka K, Sata M, Hirata Y, Nagai R. Diverse contribution of bone marrow cells to neointimal hyperplasia after mechanical vascular injuries. Circ Res. 2003; 93:783–790. [PubMed: 14500338]
49. Filip AM, Klug J, Cayli S, Frohlich S, Henke T, Lacher P, Eickhoff R, Bulau P, Linder M, Carlsson-Skwirut C, Leng L, Bucala R, Kraemer S, Bernhagen J, Meinhardt A. Ribosomal protein s19 interacts with macrophage migration inhibitory factor and attenuates its pro-inflammatory function. J Biol Chem. 2009; 284:7977–7985. [PubMed: 19155217]

CLINICAL PERSPECTIVE

Carotid intima-media thickening (IMT) is a highly predictive risk factor for cardiovascular events including myocardial infarction and stroke. Genetic models have been useful in determining causative genes that regulate carotid IMT and atherosclerosis, although much has yet to be discovered. Our genetic and bioinformatic study provides new insights into genetic pathways and a target gene, ribosomal protein L17 (RpL17), which regulate carotid intima formation. Ribosomal proteins can demonstrate extra-ribosomal roles outside of the translational machinery to control cell growth. In diseases such as Diamond Blackfan anemia as well as colorectal and gastric cancers deficiency in specific ribosomal proteins leads to malignancy. Currently, ribosomal proteins are being considered for potential therapeutic strategies to limit uncontrolled cell growth and reduce tumor size. A major contributing factor to vascular remodeling associated with IMT is increased proliferation of vascular smooth muscle cells. Thus, targeting RpL17 expression in the vascular wall may have therapeutic implications for limiting intimal hyperplasia and potential applications in the study of angiogenesis and tumor biology.

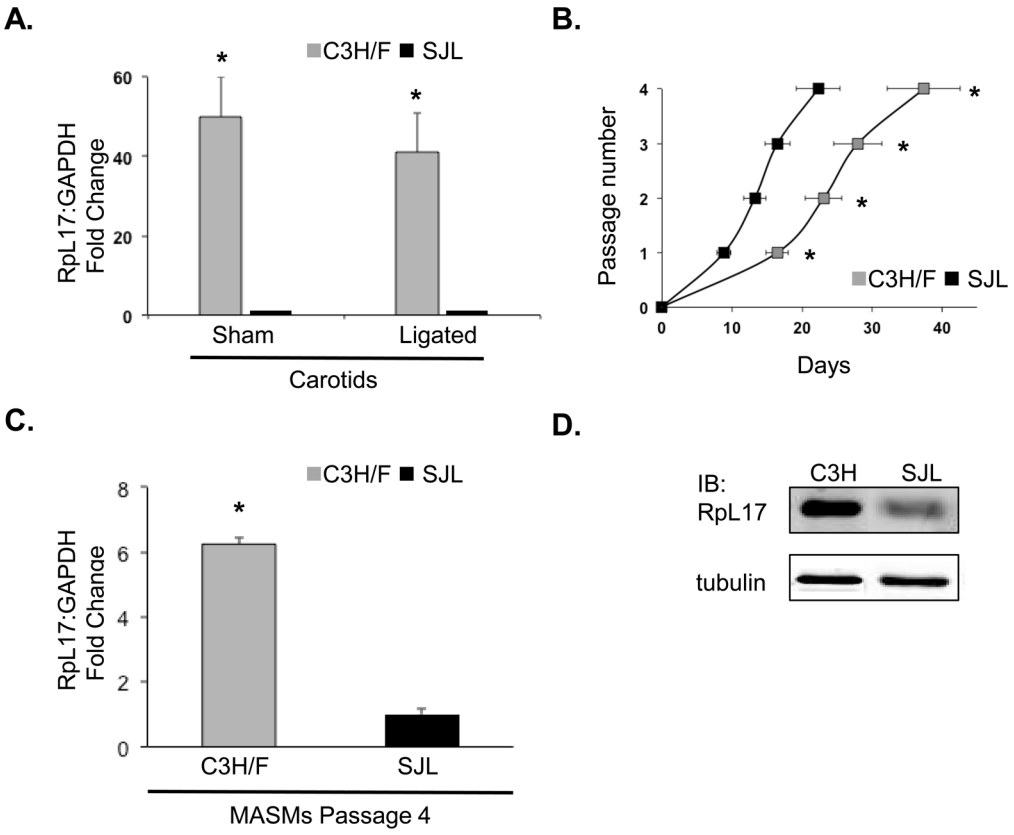

Fig. 1. Strain dependent differences in RpL17 expression

A. qRT-PCR measurement of RpL17 expression normalized to GAPDH in carotids. RpL17 is significantly up-regulated in C3H/F compared to SJL in both sham and ligated carotids. **B.** *In vitro* MASMC model for C3H/F and SJL. C3H/F MASMC grow significantly slower compared to SJL (n=13 for both C3H/F and SJL). **C.** qRT-PCR validation of RpL17 expression normalized to GAPDH in MASMC at passage 4. C3H/F MASMC have significantly greater levels of RpL17 compared to SJL, n=3. **D**. Validation of RpL17 protein expression. There was greater RpL17 protein expression in C3H/F MASMC at passage 4 compared to SJL MASMC, n≥3. Values are mean±SEM. *, $p<0.05$.

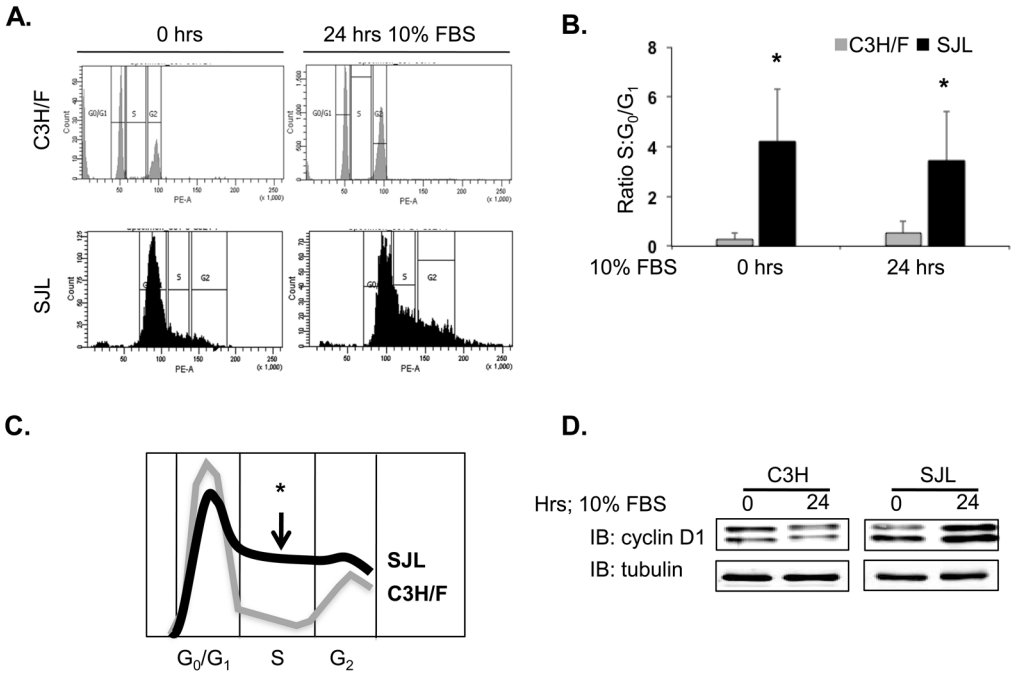

Fig. 2. Cell cycle analysis of MASMC

A. Representative flow cytometry of propidium iodide staining for C3H/F (gray) and SJL (black) MASMC. **B.** The ratio of percentage of cells in S phase compared to G_0/G_1 phase was greater in SJL compared to C3H/F MASMC. **C.** Representation of main difference in S phase (arrow) between SJL (black line) compared to C3H/F (gray line). **D.** Representative immunoblots of cyclin D1 at 0 and 24 hrs after 10% serum stimulation. Cyclin D1 expression was dramatically increased in SJL compared to C3H/F MASMC, n≥3. (Note that blots in Fig. 1D were reprobed for Cyclin D1; tubulin, as a loading control, was the same for both Figs. 1 and 3.) Values are mean±SEM. *, $p<0.05$.

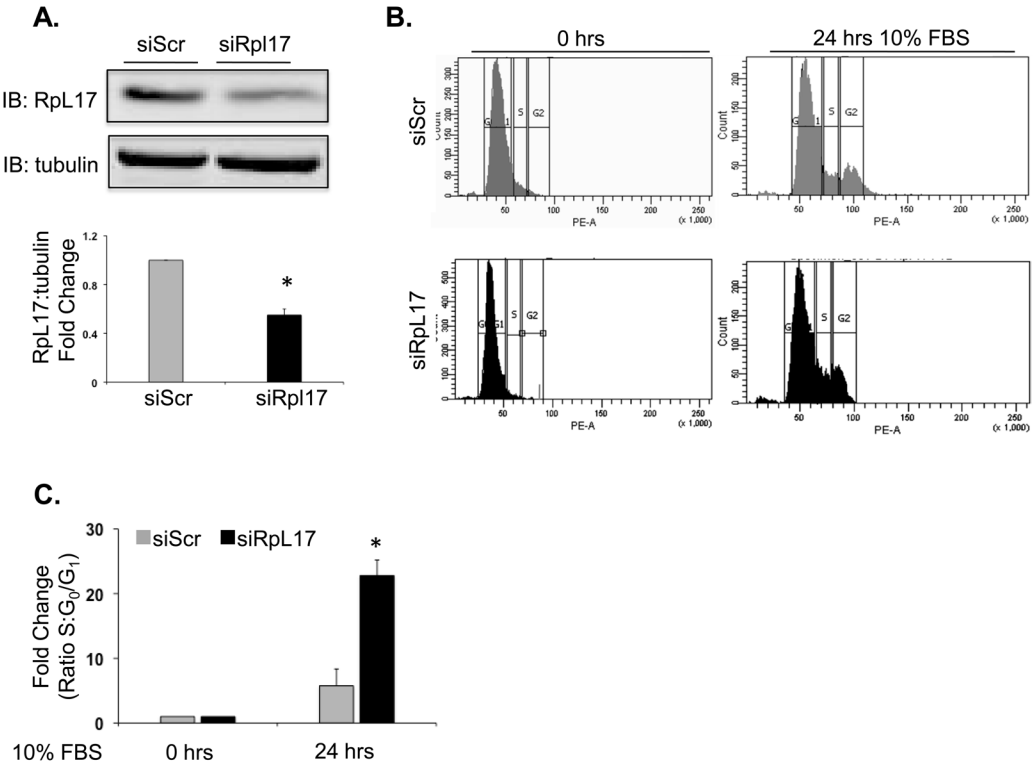

Fig. 3. Effect of RpL17 depletion on cell cycle in RASMC

A. Representative immunoblot of RpL17 in RASMC after transfection with siScr and siRpL17. Ratio of RpL17 to tubulin expressed as fold change relative to siScr is shown in bar graph. There was a significant ~50% decrease in RpL17 expression with siRpL17. **B.** Representative flow cytometry of propidium iodide staining for siScr (gray) and siRpL17 (black) in RASMC. **C.** There was an increases in the ratio of cells in S phase compared to G_0/G_1 phase at 24 hrs compared to 0 hrs after RpL17 depletion, n≥3. Values are mean ±SEM. *, $p<0.05$.

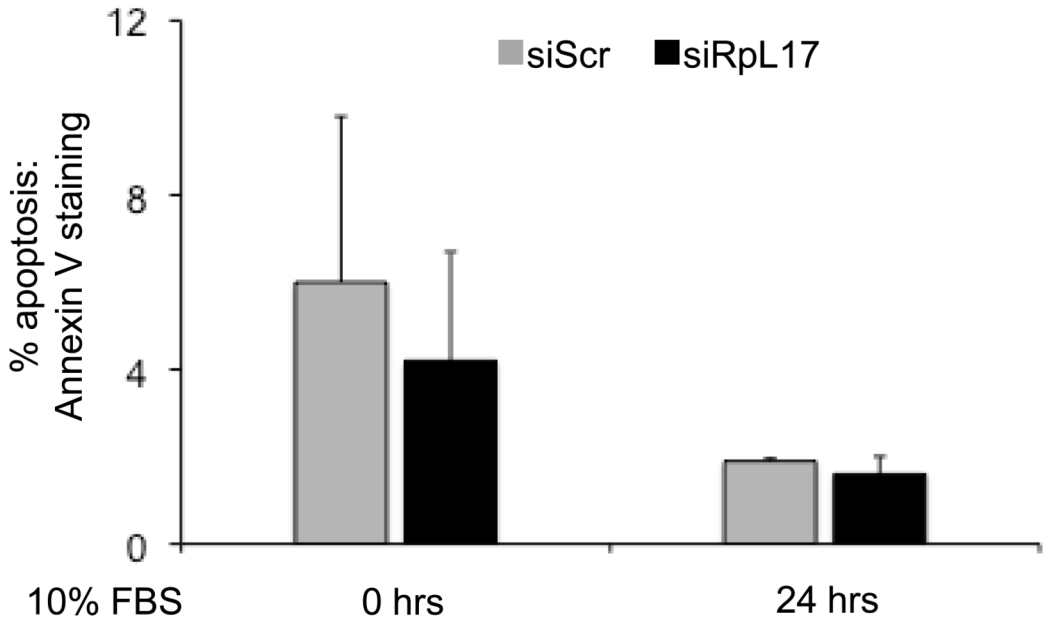

Fig. 4. RpL17 depletion on apoptosis in RASMC

Quantified flow cytometry for propidium iodide and Annexin V staining in RASMC after transfection with siScr and siRpL17. There were no differences in cell apoptosis between siScr and siRpL17 at baseline (0 hrs) or after 24 hrs serum stimulation, n≥3.

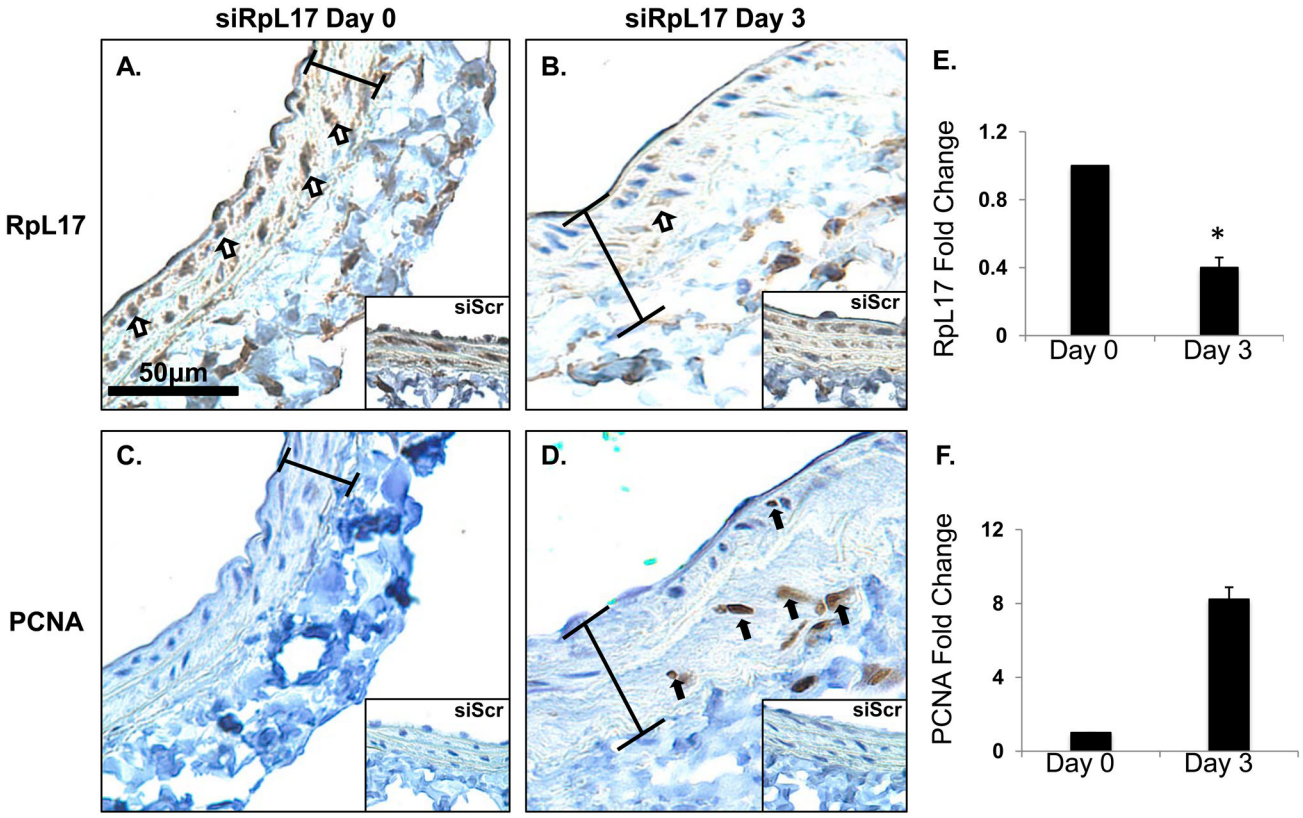

Fig. 5. RpL17 depletion in C3H/F carotid arteries

(A-B) RpL17 and (**C-D**) PCNA staining at Day 0 and 3 after pluronic gel delivery of siRpL17 to left carotid arteries in C3H/F mice. Inserts show contralateral right carotid arteries treated with siScr. The percentage of RpL17 and PCNA positive cells relative to the total number of cells in the carotid media was calculated using ImagePro Plus. RpL17 **(E)** and PCNA **(F)** expression at Day 3 after siRpL17 are graphed as fold change relative to Day 0. There was an ~2.5 decrease in RpL17 and an ~8 fold increase in PCNA in the medial area of the left carotid artery at Day 3, n≥3. Values are mean±SEM. *, $p<0.05$

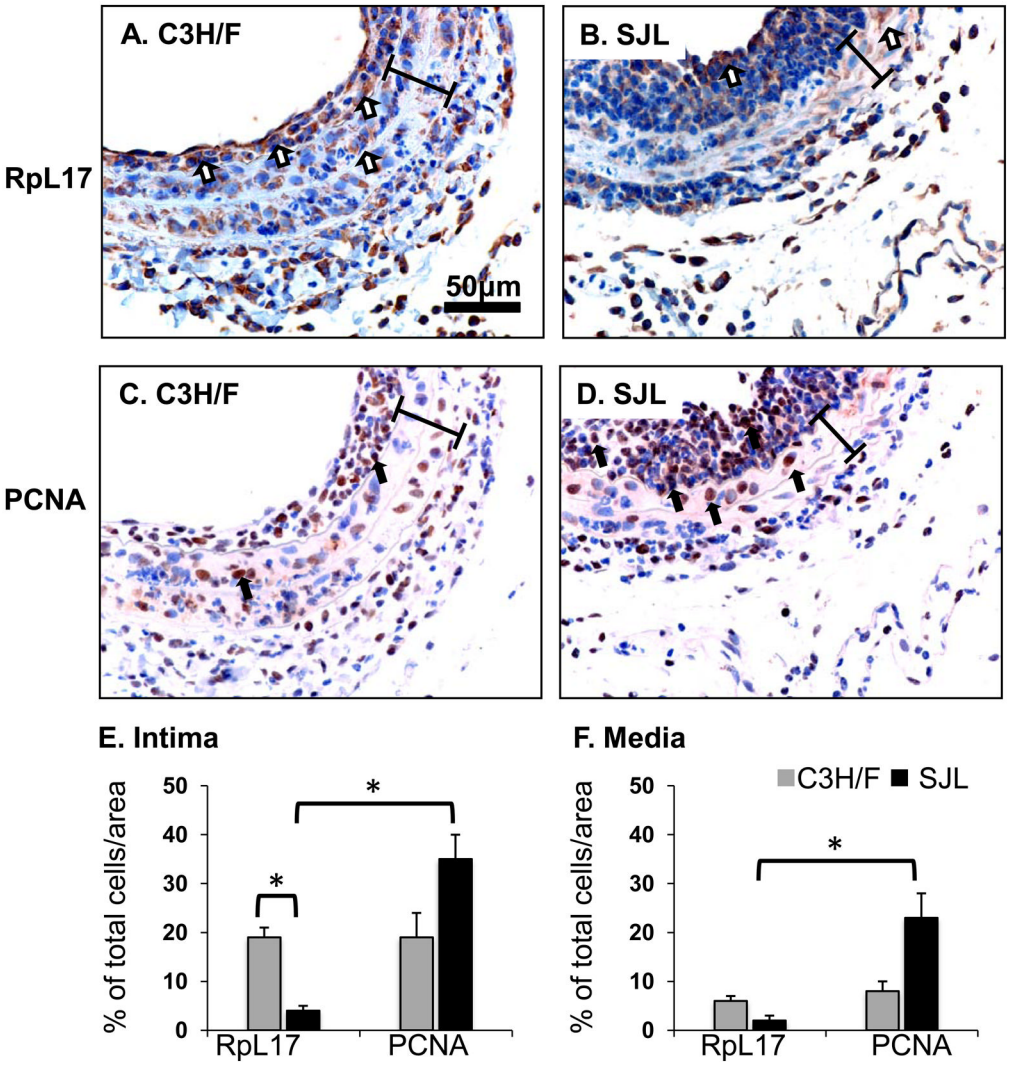

Fig. 6. RpL17 immunostaining in initma of carotid arteries following partial carotid ligation

Left carotid arteries from C3H/F and SJL were harvested 7 days after partial ligation. Serial sections were stained for (**A-B**) RpL17 and (**C-D**) PCNA. The number of RpL17 expressing cells relative to total cell number is greater in C3H/F compared to SJL (compare open arrows in A and B). PCNA expressing cells, however, are greater in SJL compared to C3H/F (compare solid arrows in C and D). **E-F.** Percentage of RpL17 and PCNA expressing cells in the intima (gray bars) and media (black bars). The percentage of RpL17 expressing cells was greater in C3H/F compared to SJL in both the intima and media. Conversely, the percentage of PCNA expressing cells was significantly higher in the intima and media in SJL compared to C3H/F carotids, n≥3. Values are mean±SEM. *, $p<0.05$.

Table 1

List of pathways that differ between carotids C3H/F versus SJL based on KEGG

b KEGG Category	KEGG Sub-Category	KEGG Pathway differed (p<0.01)
1. Metabolism (11 sub- categories)	1.1 Carbohydrate Metabolism	Pentose and glucuronate interconversions
	1.3 Lipid Metabolism	Starch and sucrose metabolism
	1.5 Amino Acid Metabolism	C21-Steroid hormone metabolism
	1.7 Glycan Biosynthesis and Metabolism	Lysine degradation
		Heparan sulfate biosynthesis
		Glycosylphosphatidylinositol(GPI)-anchor biosynthesis
		Glycan structures - biosynthesis 1
	1.9 Metabolism of Cofactors and Vitamins	Folate biosynthesis
	1.10 Biosynthesis of Secondary Metabolites	Alkaloid biosynthesis II
2. Genetic Information Processing (4 sub-categories)	2.1 Transcription	Basal transcription factors
	2.2 Translation	Ribosome
	2.3 Folding, Sorting and Degradation	Aminoacyl-tRNA biosynthesis
		Regulation of autophagy
4. Cellular Processes (9 sub-categories)	4.5 Immune System	Antigen processing and presentation
5. Human Diseases (5 sub-categories)	5.4 Metabolic Disorders	Type I diabetes mellitus